Dynamics of intrinsic optical bistability in two weakly interacting quantum systems

O. Guillot-Noël,* Ph. Goldner, and D. Gourier
Ecole Nationale Supérieure de Chimie de Paris (ENSCP), Laboratoire de Chimie Appliquée de l'Etat Solide, UMR-CNRS 7574, 11 rue Pierre et Marie Curie, 75231 Paris Cedex 05, France
(Received 30 July 2002; published 27 December 2002)

The dynamics of the intrinsic optical bistability (IOB) in an elementary quantum system is investigated in the situation where this system is composed of two weakly interacting subsystems. Numerical calculations have been performed for two ''real'' systems where IOB has been experimentally observed. The first situation corresponds to the electron-nuclear spin system of β-Ga_2O_3, where the transition between electron spin states exhibit a strong bistability. The other situation corresponds to optical transitions in Yb^{3+} pairs in $CsCdBr_3$:Yb compound, where IOB has been experimentally observed. It is shown that, in addition to the classical hysteresis of the response of the system upon variation of the power of the external field, the observation of the so-called critical slowing down is a clear signature of IOB.

DOI: 10.1103/PhysRevA.66.063813 PACS number(s): 42.65.Pc, 42.50.Md, 71.10.Li

I. INTRODUCTION

Increasing interest has been paid during the past ten years to the problem of intrinsic or mirrorless optical bistability at atomic or molecular scale [1–4]. This phenomenon, which would find application in the dynamical optical treatment and manipulation of information, manifests itself by an hysteresis of the optical response of the system upon switching up and down a control parameter, such as the incident laser intensity for example. We have presented in a previous work the general conditions that a system *S*, composed of two weakly interacting subsystems *L* and *K*, has to fulfill to exhibit an intrinsic optical bistability (IOB) [5,6]. The important condition is that the interaction *V* between the two subsystems must fluctuate with a correlation time $\tau_c \ll \hbar/V$ which measures the time during which the two subsystems retain the memory of their mutual interaction. This condition leads to a renormalization (a shift) of the resonance frequency of the probed optical transition, which means that the frequency of the transition changes continuously during the interaction with the external field. All the elementary systems which are described in such way can in principle exhibit a bistable behavior under the condition $|\Delta\omega_L^{\max}| > 2\Gamma_h$, which means that the maximum shift of the frequency ($\Delta\omega_L^{\max}$) has to be larger than the homogeneous linewidth of the transition (Γ_h). To illustrate this behavior, the line shape of the optical response (absorption or fluorescence) of a system is plotted in Fig. 1 in the case of a monostable system [case (i), discontinuous line] and in the case of a bistable system [case (ii), full line]. In the usual monostable case, the optical response of the system is the same whether the frequency is swept upwards or downwards. In the bistable case, under the condition $|\Delta\omega_L^{\max}| > 2\Gamma_h$, the line shape is bent and the response becomes dependent on the frequency sweep direction with a hysteresis window limited by abrupt transition at $\omega^{\uparrow}$ and $\omega^{\downarrow}$ between the two stable states α and γ. Under steady-state conditions, the unstable state β can never be recorded.

The general condition $|\Delta\omega_L^{\max}| > 2\Gamma_h$ can be rationalized with a ''phase diagram'' which seems to accurately predict the type of systems which could exhibit an IOB phenomenon [5]. Indeed, in the microwave range, corresponding to EPR spectroscopy (transitions between electron spin states), all the compounds which are placed in the bistable domain of the phase diagram exhibit experimentally an IOB phenomenon: i.e., β-Ga_2O_3 [6], InP [7] and metallic lithium [8]. In β-Ga_2O_3 for example, the *L* system is composed of unpaired electron spins in oxygen vacancies, the *K* system is the nuclear spins of the ^{69}Ga and ^{71}Ga nuclei and the interaction *V* between these two subsystems is an hyperfine interaction. In the near infrared and visible range corresponding to transitions between electron states, the phase diagram predicts the absence and the existence of bistable luminescence of the symmetric and asymmetric ytterbium pairs in $CsCdBr_3$, which has been experimentally observed by Helhen *et al.* [1]. In this case the two subsystems *L* and *K* are the two Yb^{3+} ions of the pairs, the interaction between these two ions could be of exchange type.

In our previous work [5], we have studied the steady-state solutions of the kinetic equations characteristic of the *L* sys-

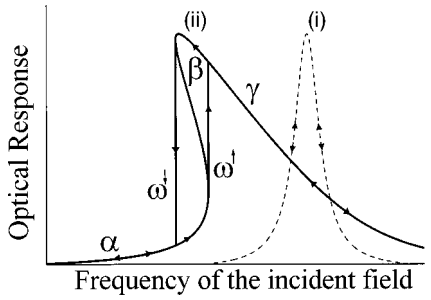

FIG. 1. Optical response of a two-level system versus the frequency ω of the external field. Case (i) corresponds to a monostable situation. The system possesses only one stable state. Case (ii) corresponds to a bistable situation with a ''shark fin'' shape transition. The system possesses two stable steady states (α, γ) and one unstable steady state β.

*Author to whom correspondence should be addressed; electronic address: guillotn@ext.jussieu.fr

tem. In the present work, we focused our attention on the dynamic processes of the IOB phenomenon. The aim of this paper is to analyze the dynamic of the bistability in order to find an experimental ''finger print'' of a bistable behavior. Numerical simulation shows the presence of a ''critical slowing down'' in the time evolution of the bistable system. The ''critical slowing down'' is the signature of the unstable β solution, which implies that there are at least two other stable steady states α and γ. It is thus not seen in the monostable situation.

This paper is decomposed as follows. In Sec. II, we briefly introduce the effective spin-Hamiltonian approach developed in Ref. [5]. We focus on two different L and K subsystems which can be characterized by either different relaxation time, by studying the case of electron and nuclear spins of β-Ga_2O_3 in the microwave range (EPR spectroscopy), or by identical relaxation time with the case of optical transitions of asymmetric ytterbium ion pairs in $CsCdBr_3$. In Sec. III, we analyze and discuss the solutions of the kinetic equation.

II. THEORETICAL BACKGROUND

The effective spin-Hamiltonian of the whole S system interacting with an electromagnetic field is written as

$$H=\hbar\omega_L L_z+\hbar\omega_K K_z+V+V'(t), \tag{1}$$

where the pseudo-Zeeman terms $\hbar\omega_L$ and $\hbar\omega_K$ correspond to the energy of the optical transitions in each subsystem. Indeed, as we focus on a particular transition by applying an electromagnetic field with angular frequency ω in quasiresonance with the probed transitions, the two subsystems L and K can be described by effective spins $L,K=\frac{1}{2}$. V is the interaction between the two subsystems. The term $V'(t)$ in Eq. (1) represents the interaction between the atomic system and the classical incident electromagnetic field. If the incident field is applied on the L subsystem, and if only the resonant terms are taken into account, V' is written as

$$V'(t)=\frac{1}{2}\hbar\Omega_1(L_+e^{-i\omega t}+L_-e^{i\omega t}), \tag{2}$$

where Ω_1 is the Rabi frequency. In the case of an electric-dipole transition, the Rabi frequency is $\Omega_1=d\xi/\hbar$, where d is the electric dipole moment and ξ the amplitude of the oscillating electric field in the slowly varying envelope approximation $(\dot{\xi}/\xi=0)$.

The time evolution of S is obtained by solving the von Neumann equation

$$\frac{d}{dt}\sigma^S(t)=\frac{1}{i\hbar}[H,\sigma^S(t)], \tag{3}$$

where σ^S is the density matrix operator of the whole system S.

Under the condition $\tau_c\ll\hbar/V$, each system can be isolated from the other and the interaction is taken into account via an average interaction [5,6]. During the time scale of the evolution of L and K, the contribution of the correlation terms between these two subsystems is neglected and σ^S can be factorized as follows:

$$\sigma^S(t)=\sigma^L(t)\otimes\sigma^K(t), \tag{4}$$

where $\sigma^L(t)$, $\sigma^K(t)$ are the reduced density matrix operators of the L and K subsystems, respectively [5].

Under the condition $\tau_c\ll\hbar/V$, applying an electromagnetic field on the L system, under the condition $\tau_c\ll\Omega_1^{-1}$ and in the quasiresonant approximation, the following kinetic equations are obtained in the case of two different L and K systems [5]:

$$\frac{d\langle L_z\rangle}{dt}=-\frac{1}{T_1^L}(\langle L_z\rangle-\langle L_z\rangle^0)+\frac{1}{T_1^{LK}}(\langle K_z\rangle-\langle K_z\rangle^0)+\frac{i\Omega_1}{2}(\langle L'_-\rangle-\langle L'_+\rangle), \tag{5}$$

$$\frac{d\langle L'_+\rangle}{dt}=+i\left(\omega_L-\omega+\frac{\langle V\rangle}{\hbar}\langle K_z\rangle\right)\langle L'_+\rangle-\frac{1}{T_2^L}\langle L'_+\rangle-i\Omega_1\langle L_z\rangle, \tag{6}$$

$$\frac{d\langle K_z\rangle}{dt}=-\frac{1}{T_1^K}(\langle K_z\rangle-\langle K_z\rangle^0)+\frac{1}{T_1^{LK}}(\langle L_z\rangle-\langle L_z\rangle^0), \tag{7}$$

where $L'_\pm=L_\pm e^{\pm i\omega t}$. The procedure and basic assumptions that are made to obtain Eqs. (5)–(7) as well as their range of validity are presented in details in Ref. [5]. The quantum mechanical average of L_z, K_z, L_+, and K_+, are respectively linked to the population inversion between the two levels and to the off-diagonal element of the density matrix: $\langle L_z\rangle$, $\langle K_z\rangle=\frac{1}{2}(\sigma_{bb}^{L,K}-\sigma_{aa}^{L,K})$, and $\langle L_+\rangle$, $\langle K_+\rangle=\sigma_{ab}^{L,K}$. The subscripts a and b refer to the ground and excited state, respectively. $\langle L_z\rangle$ and $\langle K_z\rangle$ represent the polarization of the effective spin L and K, respectively. In Eqs. (5) to (7), the terms $1/T_1^L$, $1/T_1^K$, $1/T_2^L$, and $1/T_2^K$ are the longitudinal $(1/T_1)$ and transverse $(1/T_2)$ relaxations rates of the L and K systems, respectively. $1/T_1^{LK}$ is the relaxation rate induced by the interaction V between the two subsystems. T_1^{LK} is linked to T_1^K via the leakage factor f as follows [6]:

$$T_1^{LK}=\frac{T_1^K}{f}, \tag{8}$$

where f characterizes the efficiency of the polarization transfer from the effective spin L $(\langle L_z\rangle)$ to the effective spin K $(\langle K_z\rangle)$, with $0\leq f\leq 1$. The relaxation terms T_1^L and T_1^K represent the lifetimes of the excited state associated to the L and K subsystems, respectively. T_2^L and T_2^K are linked to the homogeneous linewidth Γ_h^L and Γ_h^K of the transition by $\Gamma_h^L=1/\pi T_2^L$ and the equivalent expression for K. $\langle V\rangle$ is the mean value of the fluctuating interaction. $\langle L_z\rangle^0$ and $\langle K_z\rangle^0$ are the polarization at thermal equilibrium associated to the L and K systems, respectively, and ω_L is the frequency of the transition under study.

To generate a bistable phenomenon, a feedback loop and a nonlinear process are necessary. These two conditions are gathered in Eqs. (5) and (7). Indeed, the non linear process is due to the interaction V and is represented by the term $(\langle V\rangle/\hbar)\langle K_z\rangle\langle L'_+\rangle$ in Eq. (6), as originally discussed in Ref. [2]. The feedback loop is obtained by the combination of these equations. Without any external field, $\langle L_z\rangle=\langle L_z\rangle^0$. By exciting the L system, $\langle L_z\rangle$ becomes different from $\langle L_z\rangle^0$, a polarization transfer occurs from the L system to the K system via Eq. (7), and $\langle K_z\rangle$ becomes different from $\langle K_z\rangle^0$. As $\langle K_z\rangle$ is changing by exciting the L system, the frequency of this system changes via the $(\langle V\rangle/\hbar)\langle K_z\rangle$ term in Eq. (6). The absorption of the L system varies as the frequency of the external field is fixed and then $\langle L_z\rangle$ changes. $\langle L_z\rangle$ is thus a function of itself which gives rise to the feedback loop.

III. DYNAMICS OF IOB APPLIED TO REAL SYSTEMS

In this part we apply the previous model to real systems. Two cases are considered for which almost all parameters are known: (a) EPR transitions in the microwave range, with the example of the *n*-type semiconductor gallium oxide (β-Ga_2O_3) where the two different L and K subsystems correspond to electron and nuclear spin systems, respectively, with different relaxation times [6,7], and (b) transitions in the near infrared or visible range with the Yb^{3+} asymmetric pairs in $CsCdBr_3$, which corresponds to two different L and K subsystems (the two Yb^{3+} ions) with identical relaxation times [5]. All the differential equations are solved by using a third order Runge-Kutta method.

In the spin system of gallium oxide, the L subsystem corresponding to the unpaired electron spins located in oxygen vacancy, is characterized by an electron spin lattice relaxation time $T_1^L=2\times10^{-7}$ s and an electron spin-spin relaxation time $T_2^L=2\times10^{-7}$ s [6,7]. For the K system associated to the nuclear spin of the two ^{69}Ga and ^{71}Ga nuclei, $T_1^K=4.5\times10^{-4}$ s [6,7]. The relaxation times of the L and K subsystems differ by three orders of magnitude. The efficiency of spin-spin polarization coupling has previously been determined to be very high in the Ga system resulting in a value of the leakage factor f equals to 0.9, which leads to $T_1^{LK}=5\times10^{-4}$ s [6,7]. In β-Ga_2O_3, the L system interacts with N equivalent nuclear spins K via an hyperfine interaction A, which gives $\langle V\rangle=NA$. In EPR spectroscopy, $\langle V\rangle$ is expressed in G, with $\langle V\rangle=NA/g\beta$ where β is the Bohr magneton and g is the g factor of the unpaired electron $g=1.963(5)$ [6,7]. If we take $|\Delta\omega_L^{\max}|=5$ G (see Ref. [7]) then $\langle V\rangle=5555$ G. The Rabi frequency Ω_1 of the transition is linked to the incident microwave power by $\Omega_1=g\beta\sqrt{P/K}$ where $K=500$ is a constant characteristic of the EPR cavity. The thermal equilibrium electronic polarization $\langle L_z\rangle^0$, which amounts -10^{-3} at ambient temperature is much larger than the thermal equilibrium nuclear polarization $\langle K_z\rangle^0=10^{-6}$.

In the case of the atomic pair system (Yb^{3+} pair), we have already discussed in Ref. [5] the values of the different parameters appearing in Eqs. (5)–(7) for the case of an asymmetric pair of ytterbium in $CsCdBr_3$ host. In the present paper we take $T_1^L=T_1^K=7.8\times10^{-4}$ s, $T_2^L=1.8\times10^{-11}$ s

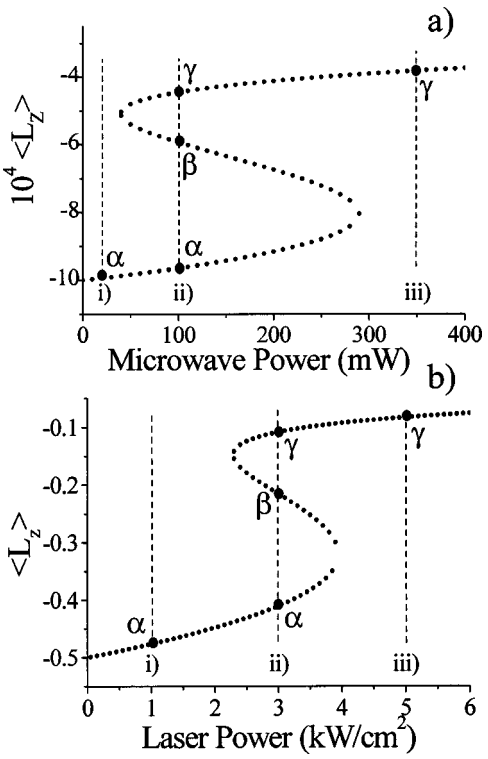

FIG. 2. Power induced-hysteresis in two IOB systems: (a) the electron-nuclear spin system (EPR transition in the microwave range) of β-Ga_2O_3; (b) the asymmetric Yb^{3+} pair system (optical transition) in $CsCdBr_3$. For β-Ga_2O_3, the parameters of the simulation are $T_1^L=T_2^L=2\times10^{-7}$ s, $T_1^K=4.5\times10^{-4}$ s, $f=0.9$, $T_1^{LK}=5\times10^{-4}$ s, $\langle V\rangle=5555$ G. For the Yb^{3+} ion pairs, $T_1^L=T_1^K=7.8\times10^{-4}$ s, $T_2^L=1.8\times10^{-11}$ s, $f=0.6$ then $T_1^{LK}=1.3\times10^{-3}$ s, $\langle V\rangle=6.66$ cm^{-1}. Three cases are considered: when the system is monostable on the α [case (i)] and γ [case (iii)] branch, and when the system is bistable with two stable steady states α and γ and one unstable steady state β [case (ii)]. For β-Ga_2O_3, cases (i), (ii), and (iii) correspond to an external microwave power of 20 mW, 100 mW, and 350 mW, respectively. For Yb^{3+} pairs, cases (i), (ii), and (iii) correspond to an external density excitation of 1000 W/cm^2, 3000 W/cm^2, and 5000 W/cm^2, respectively.

which corresponds to $\Gamma_h=0.6$ cm^{-1}, $f=0.6$, then $T_1^{LK}=1.3\times10^{-3}$ s, $\langle V\rangle=6.66$ cm^{-1}, and $|\Delta\omega_L^{\max}|=2$ cm^{-1} [5]. The power P of the incident field absorbed by the L system is linked to the Rabi frequency Ω_1 by $P=(mc\epsilon_0/q^2)(\hbar\omega_L/F_{ab})\Omega_1^2$ where F_{ab} is the oscillator strength of the transition, m and q the electron mass and charge and ϵ_0 the vacuum permittivity. We take $F_{ab}=10^{-7}$ and $\omega_L=9600$ cm^{-1} [5]. At low and ambient temperature, all the population of the L and K subsystems is in the ground state which gives $\langle L_z\rangle^0=\langle K_z\rangle^0=-0.5$.

When the system is driven under bistable conditions, the two control parameters ω and P of the incident field can produce a bistable response. In the following we only focus on the power P-induced hysteresis. Figures 2(a) and 2(b) gather the calculated curves of $\langle L_z\rangle=f(P)$, showing a power-induced hysteresis for (a) the EPR intensity of β-Ga_2O_3 and (b) the optical transitions of asymmetric ytterbium pairs in $CsCdBr_3$. The dynamics of the system was

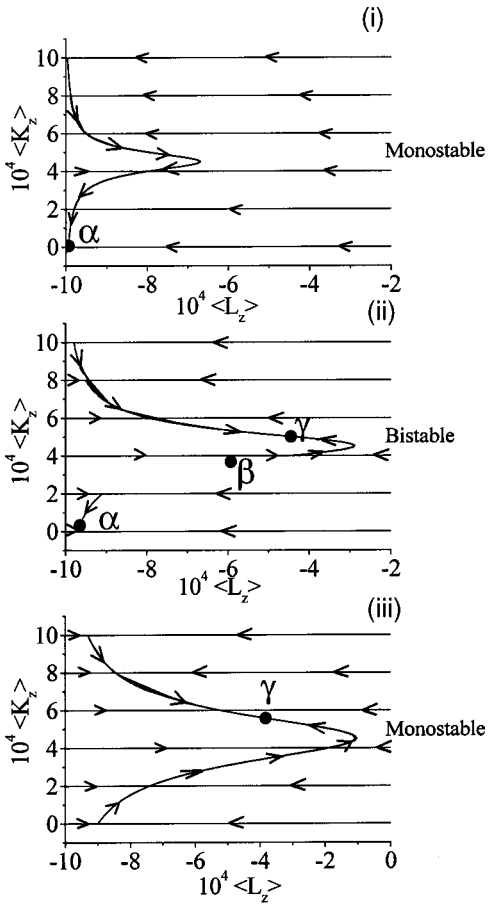

FIG. 3. Phase portrait in the $\{\langle K_z\rangle,\langle L_z\rangle\}$ space of a bistable electron-nuclear spin system. The parameters correspond to the case of the EPR transition of β-Ga_2O_3. Some trajectories generated by different initial condition $[\langle L_z(t=0)\rangle,\langle K_z(t=0)\rangle]$ are represented. The direction followed by the system is indicated by arrow on each path. The three cases discussed in Fig. 2 are shown.

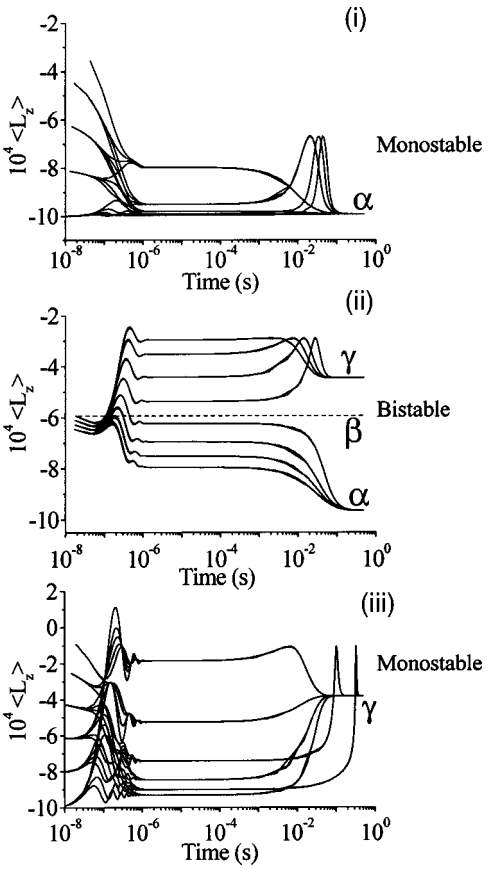

FIG. 4. Time evolution of $\langle L_z\rangle$ for the case of the electron-nuclear spin system in β-Ga_2O_3. The three cases discussed in Fig. 2 are shown.

studied by numerically solving Eqs. (5)–(7) for any initial state of the system $\langle L_z(t=0)\rangle$ and $\langle K_z(t=0)\rangle$. Three situations are considered for each case (Figs. 2) when the system is monostable with only one steady states α and γ [situations (i) and (iii)], respectively, and when the system is bistable with two stable states α and γ and one unstable state β [situation (ii)]. The initial states of the system are chosen close to the steady states α and γ and to the unsteady state β. For each initial condition, the trajectories followed by the system in phase space $\{\langle L_z\rangle,\langle K_z\rangle\}$ are gathered in Figs. 3, 4 and 5, 6 for the spin system and the atomic pair system, respectively.

The dynamics is not very sensitive to initial conditions in the electron-nuclear spin systems (Fig. 3). Indeed, all the trajectories converge towards a Lorentzian-shape trajectory which ends to the two stable steady state attractors α and γ. In the bistable case [Fig. 3(ii)], this Lorentzian-shape trajectory is cut by the unstable steady state β, which is never reached by the system. All the trajectories which passe close to β deviate from this state and converge towards α or γ [Fig. 3(ii)]. All the pathes in the phase portraits of Fig. 3 start with horizontal trajectories until they reach the Lorentzian-shape trajectory. We can thus distinguish two steps in the evolution of this system. A first step where the L system (the electron spin system) is evolving without any change in the K system (the nuclear spin system). It means that during this step we can consider that $d\langle K_z\rangle/dt=0$. A second step corresponds to the change of both subsystems. This behavior can be explain by the fact that the L system is evolving three order of magnitude faster than the K system, resulting in horizontal paths in the phase portrait of Fig. 3. After this first step, the feedback loop between the two subsystems starts to modify the trajectories, and the L and K systems are changing simultaneously, giving rise to the Lorentzian-shape trajectory in the phase space $\{\langle L_z\rangle,\langle K_z\rangle\}$. The time needed by the feedback loop to be efficient can be measured in Figs. 4(i), 4(ii) and 4(iii) which represent the evolution of $\langle L_z\rangle$ as function of time. Three time domains can be seen for each case. A first domain from $t=0$ to $t=10^{-6}$ s where the L system, which is characterized by an electron spin lattice relaxation time $T_1^L=2\times10^{-7}$ s, evolves without any change in the K system. A second domain from $t=10^{-6}$ s to $t=10^{-3}$ s characterized by a quasistationary or metastable state for the L system. During this stage, the L system transfers its polarization to the K system with a time $T_1^{LK}=5\times10^{-4}$ s. A third domain appears from $t=10^{-3}$ s to $t=10^{-1}$ s, where the K system evolves and transfers back its polarization to the L system, which starts to change again to

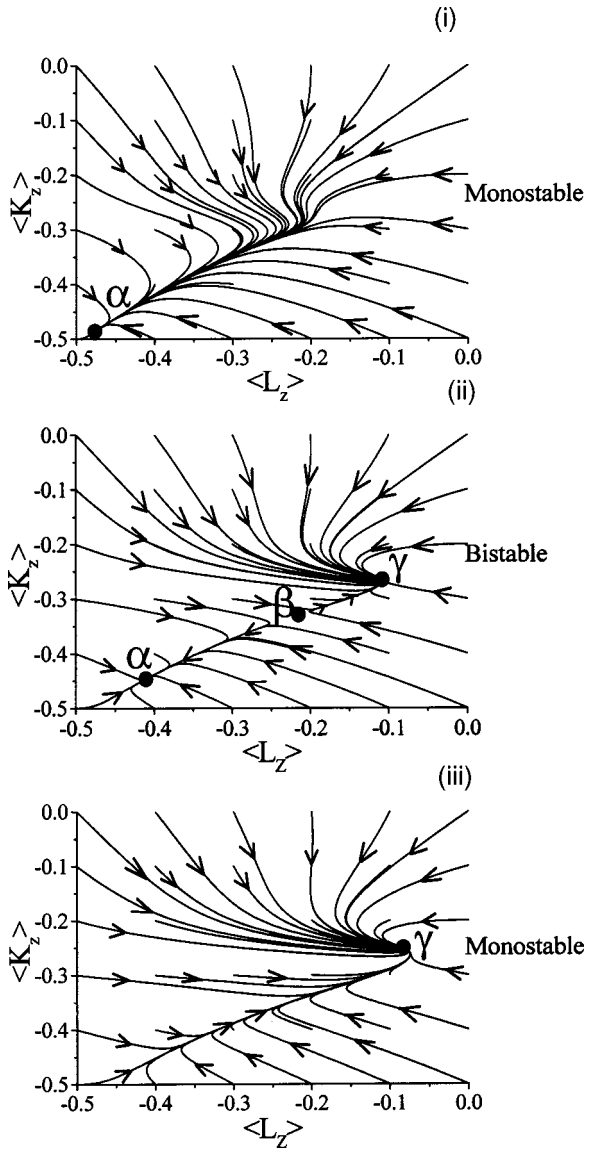

FIG. 5. Phase portrait in the $\{\langle K_z\rangle,\langle L_z\rangle\}$ space for asymmetric ytterbium pairs in $CsCdBr_3$. Some trajectories generated by different initial condition $[\langle L_z(t=0)\rangle,\langle K_z(t=0)\rangle]$ are represented. The direction followed by the system is indicated by arrows on each path. The three cases discussed in Fig. 2 are shown.

reach the stable steady states α or γ. In this time domain, the dynamic of the L system is controlled by the dynamic of the K system which evolves with a relaxation time $T_1^K=4.5\times10^{-4}$ s. From this decomposition of the dynamic evolution, it can be seen that the feedback loop needs about 10^{-3} s to link the two subsystems L and K. Whatever the initial conditions, around 0.3 s are necessary to reach the α and γ attractors.

When the two subsystems are characterized by similar relaxation times (case of Yb^{3+} pairs in $CsCdBr_3$), the feedback loop has an immediate effect on both subsystems, which evolve simultaneously as shown in Fig. 5 [monostable regimes (i) and (iii), and bistable regime (ii)]. The parameters used in these simulations are those of Fig. 2(b). All the trajectories in the phase space converge towards the attractors α or γ. Figure 6 gathers the evolution of $\langle L_z\rangle$ as function of time. Contrary to the previous system (spin systems) composed of two subsystems with very different relaxation terms, the convergence of $\langle L_z\rangle$ to the α and γ attractors is direct without any metastable state. This behavior confirms that in this case the feedback loop starts to link the two subsystems at the early beginning of the dynamic process. The stable states are reached in around 1.5×10^{-2} s [Figs. 6(i), 6(ii), 6(iii)]. It appears that when the initial conditions are close to the unstable steady state β [Fig. 6(ii)], the time needed by the system to reach the α and γ attractors is longer. For example, one trajectory in Fig. 6(ii) reaches the α state after 3×10^{-2} s, which is two times longer than the other trajectories.

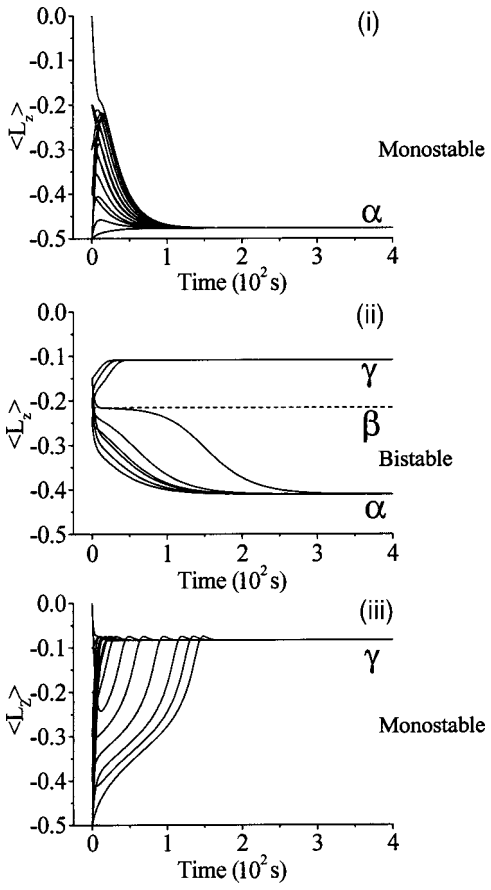

FIG. 6. Time evolution of $\langle L_z\rangle$ for the case of asymmetric ytterbium pairs in $CsCdBr_3$. The three cases discussed in Fig. 2 are shown.

In practical device using hysteresis, a bistable operation generally involves successive switching of the incident field rather than up and down slow sweeping of the control parameter. It thus appears interesting to investigate the dynamics of the two subsystems submitted to switching operations of the control parameters. In the following we study the effect of a power-field switching as it is the easiest to perform in practice. We simulate the switching operation by taking a Gaussian line shape for the switch of the external field [Figs. 7(a) and 7(b)].

The L system is prepared in a α state by sweeping the power of the external field at 100 mW in the microwave

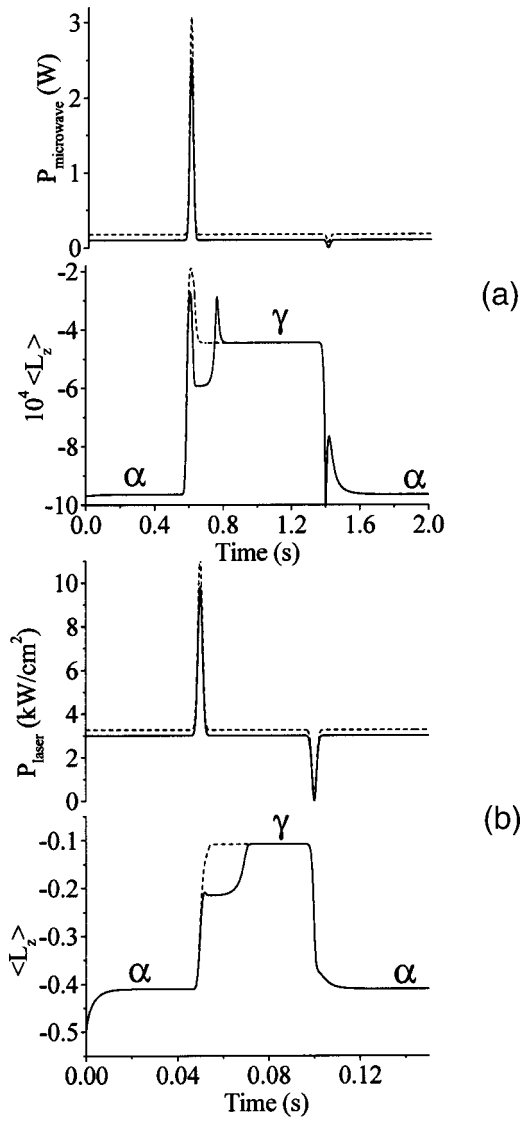

FIG. 7. Examples of power switching in (a) the electron-nuclear spin system of β-Ga_2O_3; (b) the Yb^{3+} pair system in $CsCdBr_3$. For each case, two pulses are considered: one pulse (continuous line) whose intensity corresponds to a critical power value where the L subsystem just undergoes the α to γ transition; one pulse (discontinuous line) whose intensity is higher than this critical value. For β-Ga_2O_3, $P=2.4$ W and 2.9 W for continuous and discontinuous line, respectively. The corresponding values for ytterbium pairs are $P=6850$ W/cm^2 and 8000 W/cm^2. In both cases, the pulses evolves faster than the system response with a pulse width of 10^{-2} s for β-Ga_2O_3 and 10^{-3} s for Yb^{3+} ion pairs.

range for the spin system in β-Ga_2O_3 [Fig. 7(a)] and at 3000 W/cm^2 in the infrared range for the case of the ytterbium pair system in $CsCdBr_3$ [Fig. 7(b)]. The parameters used in the simulations are those of Figs. 2(a) and 2(b). The time dependence of the external field is represented in Figs. 7(a) and 7(b) by a Gaussian line shape with a width of 10^{-2} s for the spin system and 10^{-3} s for the ytterbium pair system. The width of the pulses is chosen in such way to be one order of magnitude smaller than the time needed by the system to reach the α and γ attractors determined previously from Figs. 4 and 6. For each case, a sequence of two pulses of the incident field is considered. One is chosen in such a way that the system is driven on a trajectory of the phase portrait which passes close to the unstable steady state β (continuous line). The other one which imposes to the system a trajectory which passes far from β (discontinuous line). The pulse amplitudes are 2.4 W (full line) and 2.9 W (discontinuous line) for the spin system [Fig. 7(a)] and 6850 W/cm^2 (full line) and 8000 W/cm^2 (discontinuous line) for the ytterbium pair system [Fig. 7(b)]. As the pulses are faster than the response of the system, the pulse amplitudes have to be chosen larger than the width of the hysteresis of Figs. 2(a) and 2(b).

For β-Ga_2O_3 [Fig. 7(a)], the spin system switches from α to γ states in 0.15 s when the intense pulse is applied (discontinuous line). This is the faster switching time obtained for this system. A negative pulse of 100 mW restore the α state in 0.3 s. If the pulse is chosen in order that the system runs on a trajectory passing close to the unstable solution β (continuous line), a ''critical slowing down'' is observed in the response of the system, which switches from α to γ states in 0.3 s instead of 0.15 s. In this case, the complicated way the system reaches the steady state is a consequence of the Lorentzian line shape trajectory in the phase portrait (Fig. 3).

This critical slowing down is also seen for the case of the ytterbium ion pair system in $CsCdBr_3$ [Fig. 7(b)]. With a pulse amplitude of 8000 W/cm^2, the system switches from α to γ in 8×10^{-3} s, which is the faster switching time characteristic of this system. With a pulse amplitude of 6850 W/cm^2 [full line in Fig. 7(b)], the transition is three times longer as a consequence of the critical slowing down with a switching time of 2.4×10^{-2} s. A negative pulse of 3000 W/cm^2 restores the α state in 2×10^{-2} s.

This critical slowing down is the dynamic signature of a bistable system as it reveals the existence of the unstable steady state β and two stable steady states. Figure 8 gathers a simulation of a power switching for ytterbium pairs when the system is monostable (discontinuous line) and when it is bistable (continuous line). We obtain similar behaviors in the case of the spin system of β-Ga_2O_3. Figure 8(a) shows the response of the system as function of the power of the external laser field. In the monostable case, the response does not exhibit any hysteresis. For an excitation density of 5000 W/cm^2, the monostable system starts to saturate. In the bistable case (continuous line), the system shows an hysteresis loop with a critical power switching of 4000 W/cm^2 for the α-γ transition. The initial state of the system is characterized by $\langle L_z(t=0)\rangle=\langle K_z(t=0)\rangle=-0.5$. A rectangular pulse with an amplitude of 4000 W/cm^{-2} and a width of 0.45 s is considered. The pulse amplitude is chosen equal to the critical power switching value. If we compare the response of the system in the monostable and bistable situations, the critical slowing down is only seen in the bistable case [Fig. 8(b)]. Moreover, in the bistable situation, this behavior is very sensitive to a small change of the control parameter. Figure 8(c) shows the effect of the external power on the critical slowing down. t_{switch} in Fig. 8(c) is the time necessary for the system to reach 90% of its final state. For each point of Fig. 8(c), the initial state is $\langle L_z(t=0)\rangle=\langle K_z(t=0)\rangle=-0.5$. t_{switch} shows an abrupt change close to the critical power value of 4000 W/cm^2. Below this value the system is on the α branch of the hysteresis loop and above

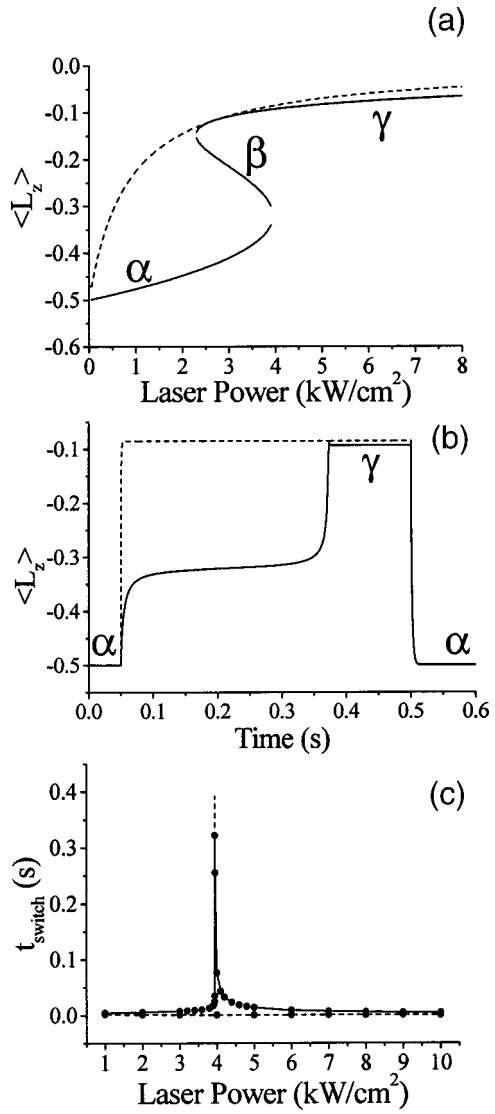

FIG. 8. The ''critical slowing down'' as a dynamic signature of a bistable system. (a) Two cases are considered for the ytterbium pair system: a monostable case (discontinuous line) and a bistable case (continuous line). A critical rectangular pulse of 4000 W/cm^2 of 0.45 s width is considered. (b) $\langle L_z \rangle$ as function of time for the monostable (discontinuous line) and bistable cases (continuous line). (c) Effect of the external power on the critical slowing down. τ_{switch} is the time needed by the system to reach 90% of its final value. The slowing down appears in a very narrow range of 50 mW/cm^2 around the critical value of 4000 W/cm^2.

this value the system is driven on the γ branch. The critical slowing down is very sensitive to the control parameters as it appears only in a very narrow range of 50 mW around the 4000 W/cm^{-2} value [Fig. 8(c)]. All the other control parameters such as the frequency of the field or internal parameters such as the leakage factor induce the same abrupt change in t_{switch} in a very narrow range around the critical value. For the γ-α transition, as the external field is switched off, the system is no longer under bistable condition and then the slowing down no longer exists [Fig. 8(b)].

IV. CONCLUSION

The dynamics of the intrinsic optical bistability has been studied by numerical simulation in the case of two weakly interacting subsystems. The important point is that, when the system is driven in a bistable situation, a critical slowing down is seen in the time response of the system when it undergoes the transition between the two steady states α and γ. These numerical simulations have been applied to real systems. The first case corresponds to EPR transitions in the electron-nuclear spin system of β-Ga_2O_3, where the two spin subsystems are characterized by relaxation time differing by three orders of magnitude. The second case corresponds to optical transitions between electronic states of ytterbium ion pairs in $CsCdBr_3$, where the two Yb^{3+} subsystems have identical relaxation time.

In the spin system case, the feedback loop connecting the electron spin system and the nuclear spin system needs a long time to operate on the two subsystems, which leads to a long switching time for the α-γ transition. In the case of Yb^{3+} pairs, the feedback loop has an immediate effect on both subsystems. The shortest switching time obtained for the α-γ transition in this case is 8×10^{-3} s.

For both cases the critical slowing down characterizes the bistable situation. This behavior is very sensitive to small variations of the control parameters. For example, in the ytterbium ion pairs system, the slowing down appears only 50 mW around an excitation density of 4000 W/cm^2.

Critical slowing down gives another signature of a bistable behavior. The combination of the steady state hysteresis loop as a function of the control parameters and of the critical slowing down constitutes a definitive proof of a bistable phenomenon. As far as this slowing down is not experimentally seen, one cannot ascertain that the observed hysteresis loop is not an experimental artifact.

[1] M. P. Hehlen, H. U. Güdel, Q. Shu, J. Rai, S. Rai, and S. C. Rand, Phys. Rev. Lett. **73**, 1103 (1994); M. P. Hehlen, A. Kuditcher, S. C. Rand, and S. R. Lüthi, *ibid.* **82**, 3050 (1999); M. P. Hehlen, H. U. Güdel, Q. Shu, and S. C. Rand, J. Chem. Phys. **104**, 1232 (1996). D. R. Gamelin, S. R. Lüthi, and H. U. Güdel, J. Phys. Chem. B **104**, 11045 (2000).

[2] C. M. Bowden and C. Sung, Phys. Rev. A **19**, 2392 (1979); C. M. Bowden, A. Postan, and R. Inguva, J. Opt. Soc. Am. B **8**, 1081 (1991); C. M. Bowden and J. P. Dowling, Phys. Rev. A **47**, 1247 (1993); C. M. Bowden and M. E. Crenshaw, Opt. Commun. **179**, 63 (2000); Y. Ben-Aryeh, C. M. Bowden, and J. C. Englund, Phys. Rev. A **34**, 3917 (1986); F. A. Hopf, C. M. Bowden, and W. H. Louisell, *ibid.* **29**, 2591 (1984); F. A. Hopf and C. M. Bowden, *ibid.* **32**, 268 (1985); M. E. Crenshaw, M. Scalora, and C. M. Bowden, Phys. Rev. Lett. **68**, 911 (1992); M. E. Crenshaw and C. M. Bowden, Phys. Rev. A **53**, 1139

(1996); M. E. Crenshaw, *ibid.* **54**, 3559 (1996).
[3] V. A. Malyshev, H. Glaeske, and K. H. Feller, Phys. Rev. A **58**, 1496 (1998); V. A. Malyshev and P. Moreno, *ibid.* **53**, 416 (1996); V. A. Malyshev, H. Glaeske, and K. H. Feller, Opt. Commun. **169**, 177 (1999); J. Chem. Phys. **113**, 1170 (2000); H. Glaeske, V. A. Malyshev, and K. H. Feller, *ibid.* **114**, 1966 (2001).
[4] J. Heber, Z. Phys. B: Condens. Matter **68**, 115 (1987); N. Bodenschatz and J. Heber, Phys. Rev. A **54**, 4428 (1996); J. Heber, J. Alloys Compd. **300–301**, 32 (2000).
[5] O. Guillot-Noël, L. Binet, and D. Gourier, Phys. Rev. B **65**, 245101 (2002).
[6] E. Aubay and D. Gourier, J. Phys. Chem. **96**, 5513 (1992); Phys. Rev. B **47**, 15023 (1993); D. Gourier, E. Aubay, and J. Guglielmi, *ibid.* **50**, 2941 (1994); D. Gerbault and D. Gourier, *ibid.* **54**, 6315 (1996); D. Gourier and D. Gerbault, *ibid.* **57**, 2679 (1998); D. Gourier, L. Binet, and D. Gerbaut, Appl. Magn. Reson. **14**, 183 (1998).
[7] L. Binet and D. Gourier, Phys. Rev. B **56**, 2688 (1997).
[8] C. Vigreux, L. Binet, and D. Gourier, J. Phys. Chem. B **102**, 1176 (1998); C. Vigreux, P. Loiseau, L. Binet, and D. Gourier, Phys. Rev. B **61**, 8759 (2000).